

Supporting Information

Pronounced, Reversible, and *in situ* Modification of the Electronic Structure of Graphene Oxide via Buckling below 160 K

Adrian Hunt^{1†}, Eamon McDermott^{1‡}, Ernst Z. Kurmaev², Alexander Moewes^{1*}*

¹Department of Physics and Engineering Physics, University of Saskatchewan. 116 Science Place, Saskatoon, Saskatchewan, S7N 5E2, Canada

² Ural Federal University, 620002, 19 Mira street, Yekaterinburg, Russia

WIEN2k Calculations

Simulation Methodology

The simulations were collected into two groups: The water/graphene simulations, which include the Hexagonal Ice and Ordered Water structures reported **Figure 2** in the main manuscript, and the deformation simulations, which included TB-Epoxy. The reported structures from each group were the least complex candidates that provided the best results from a great number of possible structures. The definition of ‘best’ is the same as that which is reported in the main manuscript: The ‘best’ structure is that which shows a reduction in the density of π^* states at 285.4 eV while showing a simultaneous increase in the density of states near 288.5 eV.

The methodology used to arrive at the optimal structure, given particular starting structure, differed somewhat between the two groups. However, there were some common points. For both groups, the optimization process was performed using settings that allowed for faster, but less accurate, simulations. This typically meant a reduction in the number of k-points, typically by an order of magnitude. In the case of the deformation simulations, $RMT \cdot k_{max}$ was also decreased by 1. Please see the later section (Simulation Parameters) for a discussion on these parameters. Once the optimization process had completed, one final optimization run was done using the final, more accurate, simulation parameters.

During force minimization calculations, spin polarized variants of the local density approximation (LDA) and the generalized gradient approximation (GGA) exchange-correlation

functionals were used for the deformation structures, but only the LDA functional was used with the water/graphene structures. Spin polarization was calculated so as to capture any dynamics brought about by the spin state of the oxygen atoms. Although the Becke-Johnson (BJ) potential would be used to calculate the final density of states, the behavior of the BJ potential during the minimization process has not been fully characterized. We therefore chose to use the typical, well-characterized functionals instead.

A) Water/graphene Structures

Given that the observed change in the graphene density of states (see Figure 1 in the main paper) occurs at low temperatures, the vast majority of the water/graphene simulations started with the intercalated water molecules positioned in the ice XI structure. The in-plane a parameter of the graphene unit cell was held constant during all simulations, although this required a small compression of the nominal ice XI unit cell. The c parameter, however, was changed to force greater or lesser interaction between the intercalating water molecules and the graphene sheets. However, this was changed by hand to study a few test cases; it was not allowed to be a free parameter within WIEN2k for the purposes of volume optimization.

The spacing between the graphene planes in the HI cell was 8.40 Å; in the OW cell, 4.43 Å. Although the volumes of the cells were kept constant during the structure optimization process, the atoms were allowed to find positions that minimized the force exerted upon them, and thus, minimize the total energy of the cell. For the ice XI-based cells, force minimization invariably disrupted the XI structure and removed whatever influence there was upon the graphene sheets. As mentioned in the main paper, the effect of ice upon the graphene density of states was negligible after force minimization, regardless of the length of the c -axis. For the water/graphene structures that did not start in an ice XI-related structure, the end result was the same: Force minimization removed any influence the water molecules may have initially had upon the electronic structure of graphene.

For the optimized Hexagonal Ice structure, all C-C bonds within the graphene sheets are the between 1.41 Å and 1.42 Å. The O-H bonds vary between 1.02 Å and 1.09 Å, depending on the location of the water molecule. The C-C bonds in the Ordered Water structure are also 1.42 Å, whereas the O-H bonds are somewhat smaller, varying between 0.97 Å and 1.03 Å.

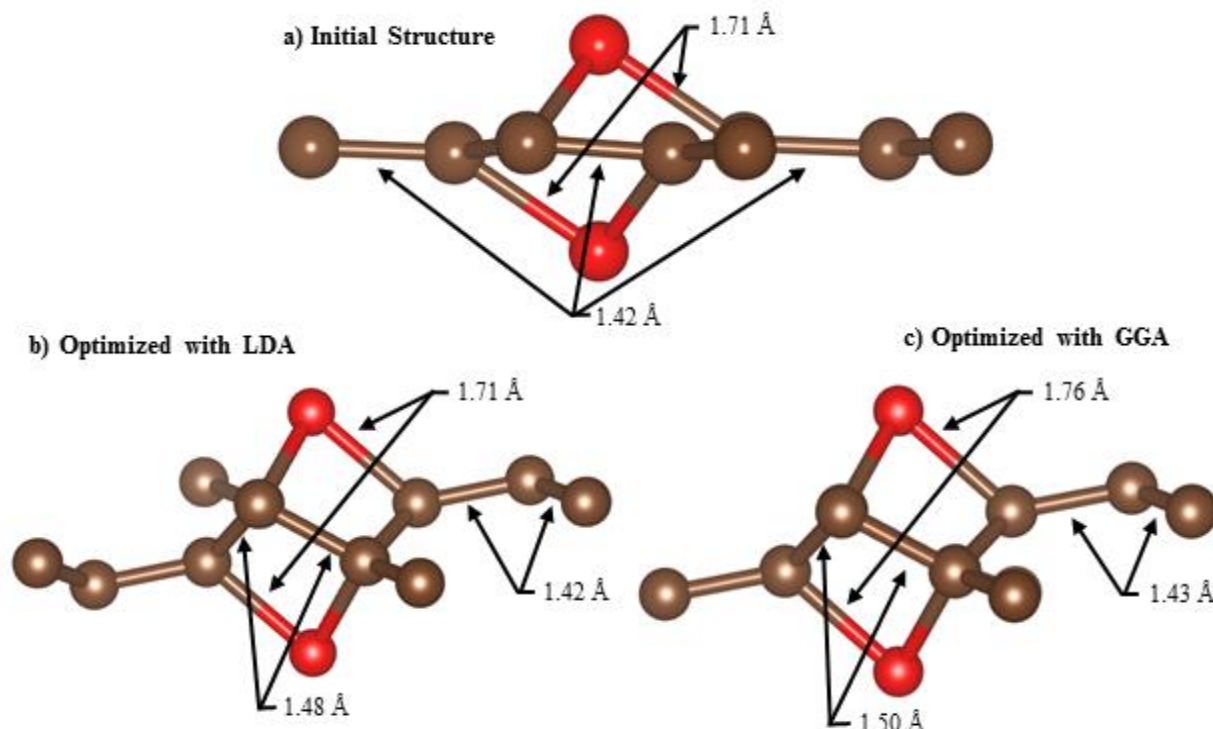


Figure S1: The evolution of the TB-epoxide structure. a) Initial guess given to WIEN2k. b) Optimized structure using spin-polarized LDA. c) Optimized structure using spin-polarized GGA. In all panels, the bond lengths are given. The fact that the C-O bond length does not change is a coincidence. Images made with VESTA.⁽⁵⁾

B) Deformation Structures

The deformation structures involved direct functionalization of the graphene via C-O bonds, so structural optimization required volume optimization as well as force minimization. This was done sequentially in the following pattern: The volume was adjusted by changing some combination of the a , b , and c axes, depending on the symmetry of the unit cell. In the case of TB-epoxide, the a and b axes were changed simultaneously by the same amount, whereas the c axis was left untouched; interplanar interaction was not a parameter that we explored in this study, so it was kept a constant 10 Å. Once the volume had been adjusted, the structure was allowed to go through a full force minimization routine to find the optimal structure for that particular unit cell volume.

As mentioned, both the spin-polarized LDA and spin-polarized GGA exchange-correlation functionals were used during the structure optimization process of the deformation structures.

GGA was used because it is more widely used during force minimization of covalently bonded structures, because LDA typically overbinds in such situations. Nevertheless, LDA was also used in order to directly compare results from the deformation structures with those from the water/graphene structures. Additionally, we have found that GGA drastically underbinds for graphite. Volume optimization calculations for graphite have shown that GGA predicts that graphite is not stable, where LDA closely predicts the appropriate, experimentally-determined interplanar spacing of 3.35 Å.

The initial structure of the TB-epoxide cell has oxygen atoms above and below the graphene plane, centered on one of the rings. The 2, 4, and 6 carbon atoms were manually pulled up out of plane slightly, while the 1, 3, and 5 carbon atoms were pulled down slightly. **Figure S1** shows the initial and optimized structures, along with the bond lengths.

Simulation Parameters

All simulations presented in the paper were performed using the WIEN2k commercial DFT code. All calculations used the Becke-Johnson (BJ) potential because it attempts to account for dispersion forces between molecules in an *ab initio* way using only the electron densities calculated by DFT.⁽¹⁾ Although this is less necessary for TB-epoxide than for Hexagonal Ice or Ordered Water, because all interactions were largely covalent, we nevertheless used the BJ potential to maintain internal consistency. As it turns out, the BJ potential most closely simulated the changes in the C 1s XAS spectra seen in **Figure 1** in the main manuscript.

Strictly speaking, the WIEN2k code uses a modified version of the Becke-Johnson potential, as described by Tran and Blaha, wherein the BJ potential is used in conjunction with LDA correlation.⁽²⁾ The modifications of Tran and Blaha were implemented with the specific goal of correctly simulating the band gap of transition metal oxide systems without introducing an external field, as is done within the LDA+U framework. However, the modifications are strictly not *ab initio* in that they introduce an additional mixing parameter, and the scaling factor of this mixing is dictated by the user. If one sets the scaling factor for the additional parameter to 0, then the original Becke-Johnson form is recovered from the modified Becke-Johnson potential. This was done for all calculations presented in the main paper.

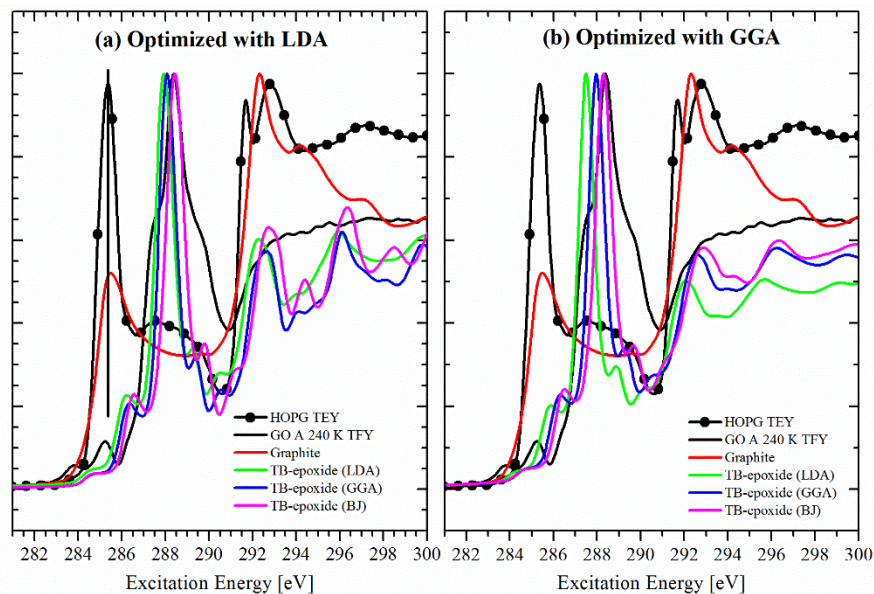


Figure S2: Comparison of simulated C 1s XANES spectra from the (a) LDA-optimized TB-epoxide structure, and (b) GGA-optimized structure, using different exchange-correlation functionals. The red curve is a simulation of graphite, which was calculated using the BJ functional. Although the BJ spectrum aligns with experiment best, the other functionals also provide good results. The GGA-optimized structure produces slightly better results above 291 eV, but the LDA-optimized results are more accurate below 291 eV.

Although the BJ potential was chosen for reasons of internal consistency so as to allow direct comparison of the water/graphene and TB-epoxide results, we did simulate the electronic structure of TB-epoxide using the LDA and GGA functionals, for both the LDA- and GGA-optimized structures. The simulated C 1s XANES spectra are shown in **Figure S2**. The BJ spectrum aligns best with the experimental spectrum taken from GO A, however, the other functionals also provide good results.

Generally speaking, the results of the two structures are very similar on the C 1s edge, particularly for the GGA and BJ functionals. As is shown in the main manuscript, results vary much more strongly on the O 1s edge. This is to be expected, given that the C-O bond distance is the greatest difference between the two structures. As it turns out, the experimental C 1s and O 1s XANES spectra are best reproduced by the BJ functional on the LDA-optimized structure.

Concerning the simulation parameters: The relevant input parameters for the simulations presented in the paper are shown in **Table S1**, which includes the number of k-points, the cut-off energy between the core and valence states, the radius of the muffin tin (RMT) around each atom type, and the product $\text{RMT} \cdot k_{\text{max}}$. The listed number of k-points are those used within the irreducible part of the Brillouin zone; the number varies between calculations simply because larger cells, and more symmetric cells, require fewer k-points for comparable levels of computational accuracy. The product $\text{RMT} \cdot k_{\text{max}}$ is the simulation parameter that most strongly influences the accuracy of the calculation, other than the number of k-points. $\text{RMT} \cdot k_{\text{max}}$ effectively determines the size of the basis set of plane waves. A larger $\text{RMT} \cdot k_{\text{max}}$ means a more accurate calculation, but at the cost of computational efficiency; the balance between the two extremes varies according to the smallest RMT in the unit cell. $\text{RMT} \cdot k_{\text{max}}$ values of 3.0 are typically a good compromise for unit cells with a very small RMT, such as is the case with the hydrogen-containing cells.⁽³⁾ Setting the $\text{RMT} \cdot k_{\text{max}}$ larger than 3.0 for the TB-epoxide cell was necessary due to the larger RMT values.

We set $\text{RMT} \cdot k_{\text{max}}$ to 8.0 specifically because this is the same value used to simulate graphite. As noted in the main text, all simulations were not shifted arbitrarily, but rather by an amount set by a known quantity. In this particular case, the simulated XANES spectrum of graphite, when calculated with an $\text{RMT} \cdot k_{\text{max}}$ of 8.0 using the BJ potential, needed to be shifted by 13.0 eV in order to line up with the experimental spectrum. Consequently, the C 1s XANES spectra from HI, OW, and TB-epoxide were all shifted by 13.0 eV.

Table S1: Input parameters for WIEN2k simulations

Parameters	Hexagonal ice (HI)	Ordered water (OW)	TB-epoxide
Number of k-points	423	1365	351
Cut-off energy [Ry]	-6.0	-6.0	-6.0
RMT: carbon [Å]	1.26	1.26	1.26
RMT: oxygen [Å]	1.12	1.12	1.26
RMT: hydrogen [Å]	0.60	0.60	N/A
$\text{RMT} \cdot k_{\text{max}}$	3.0	3.0	8.0

Calculation of Enthalpies of Formation

Table 2 in the main manuscript lists computed enthalpies of formation, ΔH° . ΔH° , for each structure, was computed according to the following formula:

$$\Delta H^\circ_{structure} = \frac{E_{total} - (N_C \cdot E_C + N_O \cdot E_O + N_H \cdot E_H)}{N_{bonds}}$$

In the formula, E_{total} is the total energy of the structure in question, N_C , N_O , and N_H are the numbers of carbon, oxygen, and hydrogen atoms, respectively, in the structure; E_C , E_O , and E_H are the total energies of unit cells containing isolated carbon, oxygen, and hydrogen atoms, respectively; and N_{bonds} is the total number of bonds. Typically, each carbon was assumed to make four bonds, each oxygen was assumed to make two bonds, and each hydrogen could make one bond. The obvious exception was TB-epoxide, wherein the oxygen atoms were assumed to make three bonds each.

The unit cells with the isolated atoms were 10 Å x 10 Å x 10 Å, with the atoms sitting at the corners. The RMT*K_{max} values were kept constant, and the muffin radii of the atoms were set to the same values as used for the simulated structures listed in **Table 2**.

Peak Assignments for Graphene Oxide Calculations

Figure 2 and **Figure 3** in the main manuscript contain results of simulations previously published, specifically, the Full GO curves.⁽⁴⁾ Unlike the other simulated spectra presented in these two Figures, the Full GO simulations are composite results from three different unit cells, which were then combined in a weighted average. For ease of reference for the reader, we show the theoretical XANES spectra, calculated from the same simulated electronic structure, in **Figure S3**. We also display peak assignments to show the origins of the features within each spectrum.

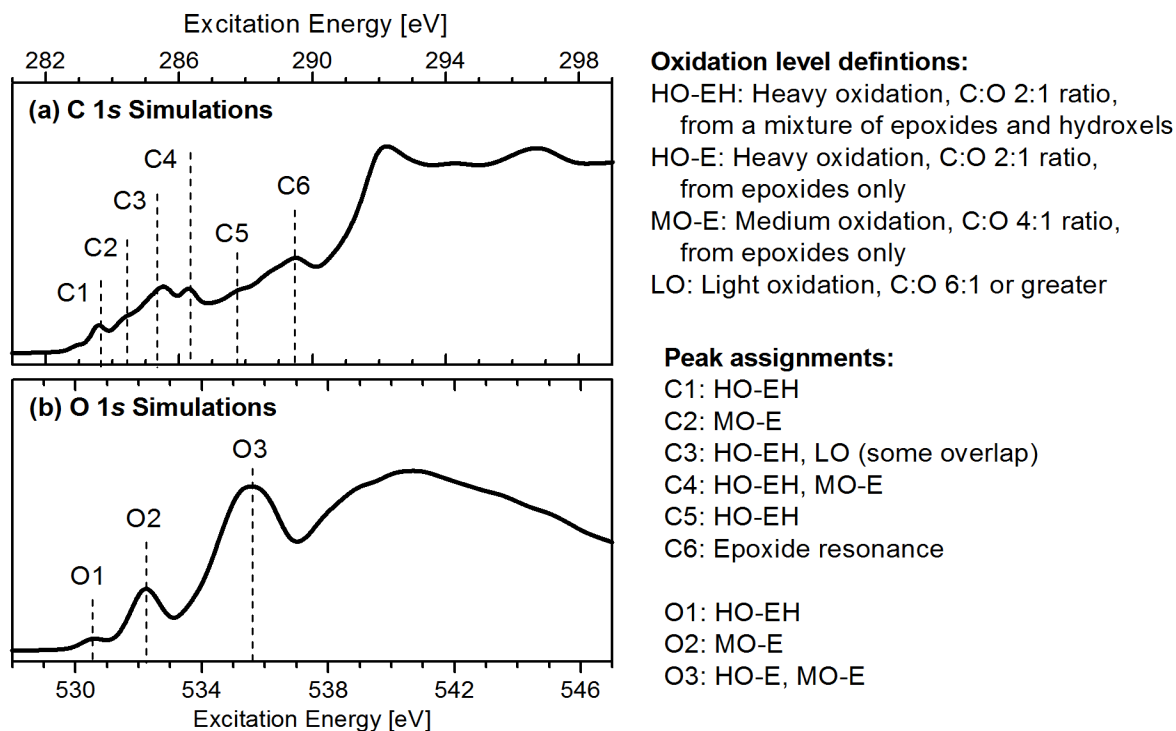


Figure S3: Peak assignments for the composite simulations first published in Ref. 4. The C 1s XANES shown in (a) and the O 1s XANES shown in (b) were both calculated using the same simulated electronic structure.

Crystal Structures

Crystallographic descriptions of each of the three structures, in CIF format, are given below.

Each of the four CIF files below were generated from the WIEN2k structure files using VESTA.⁽⁵⁾

Note that the unit cell parameters change quite substantially between the different simulations. This is due to the symmetry maximization step in WIEN2k; in the case of TB-Epoxy, the volume was also optimized. When using WIEN2k, the program automatically adjusts the unit cell given to it by the user to find an equivalent cell with the highest possible symmetry and the lowest number of non-equivalent sites. During this process, the unit cell parameters will often change. One can keep this from happening by forcing the program to accept non-equivalency, which is necessary when one wishes to calculate phenomena such as antiferromagnetism. For the work presented in this paper, however, forcing non-equivalency is not necessary, and we allowed WIEN2k to find the simplest, most symmetric representation of each unit cell possible.

1) Graphene/water: Hexagonal ice (HI)

```
_cell_length_a      4.25394
_cell_length_b      4.25394
_cell_length_c      8.40327
_cell_angle_alpha    90
_cell_angle_beta     90
_cell_angle_gamma    119.99903
_symmetry_space_group_name_H-M  'P 1'
_symmetry_Int_Tables_number      1
```

```
loop_
_symmetry_equiv_pos_as_xyz
  'x, y, z'
```

```
loop_
  _atom_site_label
  _atom_site_occupancy
  _atom_site_fract_x
  _atom_site_fract_y
  _atom_site_fract_z
  _atom_site_adp_type
  _atom_site_B_iso_or_equiv
  _atom_site_type_symbol
H1      1.0  0.000000  0.000000  0.000000  Biso  1.000000  H
H2      1.0  0.206265  0.395552  0.876761  Biso  1.000000  H
H3      1.0  0.731469  0.868082  0.199351  Biso  1.000000  H
H4      1.0  0.602803  0.792457  0.876961  Biso  1.000000  H
H5      1.0  0.135217  0.271715  0.199071  Biso  1.000000  H
H6      1.0  0.330856  0.672380  0.350317  Biso  1.000000  H
H7      1.0  0.150894  0.847084  0.870013  Biso  1.000000  H
H8      1.0  0.196828  0.806316  0.199280  Biso  1.000000  H
O1      1.0  0.003902  0.994666  0.878360  Biso  1.000000  O
O2      1.0  0.336271  0.667186  0.233058  Biso  1.000000  O
O3      1.0  0.329434  0.668761  0.900041  Biso  1.000000  O
O4      1.0  0.007268  0.995851  0.176963  Biso  1.000000  O
C1      1.0  0.334089  0.664507  0.567984  Biso  1.000000  C
C2      1.0  0.000828  0.997804  0.563731  Biso  1.000000  C
C3      1.0  0.333872  0.998321  0.565643  Biso  1.000000  C
C4      1.0  0.667625  0.331195  0.565314  Biso  1.000000  C
C5      1.0  0.667899  0.664409  0.565622  Biso  1.000000  C
C6      1.0  0.000135  0.330227  0.565553  Biso  1.000000  C
```

2) Graphene/water: Ordered water (OW)

```

_cell_length_a      2.45600
_cell_length_b      4.25391
_cell_length_c      8.86020
_cell_angle_alpha   90
_cell_angle_beta    90
_cell_angle_gamma    90
_symmetry_space_group_name_H-M  'P 1'
_symmetry_Int_Tables_number      1

```

```

loop_
_symmetry_equiv_pos_as_xyz
  'x, y, z'

```

```

loop_
  _atom_site_label
  _atom_site_occupancy
  _atom_site_fract_x
  _atom_site_fract_y
  _atom_site_fract_z
  _atom_site_adp_type
  _atom_site_B_iso_or_equiv
  _atom_site_type_symbol
  C1      1.0  0.000000  0.000000  0.000000  Biso 1.000000 C
  C2      1.0  0.523647  0.499635  0.499998  Biso 1.000000 C
  C3      1.0  0.000072  0.331358  0.000176  Biso 1.000000 C
  C4      1.0  0.523585  0.831023  0.499906  Biso 1.000000 C
  C5      1.0  0.500832  0.498079  0.000246  Biso 1.000000 C
  C6      1.0  0.022806  0.997740  0.500137  Biso 1.000000 C
  C7      1.0  0.500699  0.833314  0.000117  Biso 1.000000 C
  C8      1.0  0.022900  0.332918  0.500086  Biso 1.000000 C
  O1      1.0  0.491481  0.162222  0.756190  Biso 1.000000 O
  O2      1.0  0.471668  0.167483  0.243224  Biso 1.000000 O
  O3      1.0  0.060540  0.660498  0.743097  Biso 1.000000 O
  O4      1.0  0.039949  0.668544  0.255994  Biso 1.000000 O
  H1      1.0  0.324385  0.387380  0.751116  Biso 1.000000 H
  H2      1.0  0.285784  0.385522  0.247676  Biso 1.000000 H
  H3      1.0  0.248934  0.877531  0.747196  Biso 1.000000 H
  H4      1.0  0.211077  0.892201  0.251691  Biso 1.000000 H
  H5      1.0  0.822104  0.162191  0.695251  Biso 1.000000 H
  H6      1.0  0.769400  0.172312  0.315880  Biso 1.000000 H
  H7      1.0  0.769423  0.664394  0.817754  Biso 1.000000 H
  H8      1.0  0.715398  0.670743  0.192692  Biso 1.000000 H

```

3) TB-epoxide, optimized with spin-polarized LDA

```
_cell_length_a      4.67116
_cell_length_b      4.67116
_cell_length_c      10.00000
_cell_angle_alpha    90
_cell_angle_beta     90
_cell_angle_gamma    120
_symmetry_space_group_name_H-M  'P -3 m 1'
_symmetry_Int_Tables_number  164
```

loop_

_symmetry_equiv_pos_as_xyz

```
'x, y, z'
'-x, -y, -z'
'-y, x-y, z'
'y, -x+y, -z'
'-x+y, -x, z'
'x-y, x, -z'
'y, x, -z'
'-y, -x, z'
'x-y, -y, -z'
'-x+y, y, z'
'-x, -x+y, -z'
'x, x-y, z'
```

loop_

_atom_site_label

_atom_site_occupancy

_atom_site_fract_x

_atom_site_fract_y

_atom_site_fract_z

_atom_site_adp_type

_atom_site_B_iso_or_equiv

_atom_site_type_symbol

C1	1.0	0.838933	0.677865	0.964502	Biso	1.000000	C
C7	1.0	0.333333	0.666667	0.062288	Biso	1.000000	C
O1	1.0	0.000000	0.000000	0.147317	Biso	1.000000	O

4) TB-epoxide, optimized with spin-polarized GGA

```
_cell_length_a      4.73263
_cell_length_b      4.73263
_cell_length_c      10.00000
_cell_angle_alpha    90
_cell_angle_beta     90
_cell_angle_gamma    120
_symmetry_space_group_name_H-M  'P -3 m 1'
_symmetry_Int_Tables_number  164
```

loop_

_symmetry_equiv_pos_as_xyz

```
'x, y, z'
'-x, -y, -z'
'-y, x-y, z'
'y, -x+y, -z'
'-x+y, -x, z'
'x-y, x, -z'
'y, x, -z'
'-y, -x, z'
'x-y, -y, -z'
'-x+y, y, z'
'-x, -x+y, -z'
'x, x-y, z'
```

loop_

_atom_site_label

_atom_site_occupancy

_atom_site_fract_x

_atom_site_fract_y

_atom_site_fract_z

_atom_site_adp_type

_atom_site_B_iso_or_equiv

_atom_site_type_symbol

C1	1.0	0.838210	0.676420	0.965274	Biso	1.000000	C
C2	1.0	0.333333	0.666667	0.061438	Biso	1.000000	C
O1	1.0	0.000000	0.000000	0.150815	Biso	1.000000	O

- (1) Becke, A. D.; Johnson, E. R. A simple effective potential for exchange. *J. Chem. Phys.* **2006**, *124*, 221101.
- (2) Tran, F.; Blaha, P. Accurate band gaps of semiconductors and insulators with a semilocal exchange-correlation potential. *Phys. Rev. Lett.* **2009**, *102*, 226401.
- (3) Blaha, P.; Schwarz, K.; Madsen, G. K. H.; Kvasnicka, D.; Luitz, J. *WIEN2k, An Augmented Plane Wave + Local Orbitals Program for Calculating Crystal Properties*; Karlheinz Schwarz, Techn. Universitat Wien, Austria, 2001.
- (4) Hunt, A.; Kurmaev, E. Z.; Moewes, A. A re-evaluation of how functional groups modify the electronic structure of graphene oxide. *Adv. Mater.* **2014**, *26*, 4870–4874.
- (5) Momma, K.; Izumi, F. VESTA 3 for three-dimensional visualization of crystal, volumetric and morphology data. *J. Appl. Crystallogr.* **2011**, *44*, 1272–1276.